AGU PUBLICATIONS

Geophysical Research Letters

RESEARCH LETTER
10.1002/2014GL059971

Key Points:
- Site of newly ventilated Antarctic Bottom Water was discovered by observations
- Dense shelf water in VB polynya is dense enough to reach the bottom layer
- Transport estimates revealed a significant influence on basin bottom water

Supporting Information:
- Readme
- Figure S1

Correspondence to:
Y. Kitade,
ykitade@kaiyodai.ac.jp

Citation:
Kitade, Y., K. Shimada, T. Tamura, G. D. Williams, S. Aoki, Y. Fukamachi, F. Roquet, M. Hindell, S. Ushio, and K. I. Ohshima (2014), Antarctic Bottom Water production from the Vincennes Bay Polynya, East Antarctica, *Geophys. Res. Lett.*, *41*, 3528–3534, doi:10.1002/2014GL059971.

Received 25 MAR 2014
Accepted 11 MAY 2014
Accepted article online 14 MAY 2014
Published online 29 MAY 2014

Antarctic Bottom Water production from the Vincennes Bay Polynya, East Antarctica

Yujiro Kitade[1], Keishi Shimada[1], Takeshi Tamura[2,3], Guy D. Williams[3], Shigeru Aoki[4], Yasushi Fukamachi[4], Fabien Roquet[5], Mark Hindell[6], Shuki Ushio[2], and Kay I. Ohshima[4]

[1]Tokyo University of Marine Science and Technology, Tokyo, Japan, [2]National Institute of Polar Research, Tachikawa, Japan, [3]Antarctic Climate and Ecosystems Cooperative Research Centre, University of Tasmania, Hobart, Tasmania, Australia, [4]Institute of Low Temperature Science, Hokkaido University, Sapporo, Japan, [5]Department of Meteorology, Stockholm University, Stockholm, Sweden, [6]Institute for Marine and Antarctic Studies, University of Tasmania, Hobart, Tasmania, Australia

Abstract One year moorings at depths greater than 3000 m on the continental slope off Vincennes Bay, East Antarctica, reveal the cold (<-0.5°C) and fresh (<34.64) signals of newly formed Antarctic Bottom Water (AABW). The signal appeared in June, 3 months after the onset of active sea-ice production in the nearby Vincennes Bay Polynya (VBP). The AABW signal continued for about 5 months at two moorings, with 1 month delay at the western site further downstream. Ship-based hydrographic data are in agreement, detecting the westward spread of new AABW over the continental slope from VBP. On the continental shelf, Dense Shelf Water (DSW) formation is observed by instrumented seals, in and around the VBP during autumn, and we estimate its transport to be 0.16 ± 0.07 ($\times 10^6 m^3 s^{-1}$). We conclude that the DSW formed in this region, albeit from a modest amount of sea-ice production, nonetheless contributes to the upper layer of AABW in Australian-Antarctic Basin.

1. Introduction

Antarctic Bottom Water (AABW) is the densest water in the ocean and globally significant; its production at the Antarctic margin is a key component of the global overturning circulation [*Speer et al*., 2000; *Marshall and Speer*, 2012]. Historically, there have been three well-defined source regions in the Weddell [*Gill*, 1973] and Ross Seas [*Jacobs et al*., 1970], and off Adélie Land [*Rintoul*, 1998; *Williams et al*., 2008, 2010]. Despite extensive studies on the formation and transport processes of AABW, the estimates of total AABW volume transport range widely from 8 to 28 Sv [*Jacobs*, 2004] ($1\ Sv = 10^6\ m^3\ s^{-1}$) due to uncertainties in the estimation methods and an incomplete assessment of all potential AABW production regions. It is vital that the observational estimate of total AABW transport, a parameter critical to the global climate modeling community, is improved by ensuring all AABW source regions are identified and all mechanisms involved fully understood.

In general, AABW is produced over the continental slope and rise by the mixing of cold, DSW descending into warm Circumpolar Deep Water (CDW) [e.g., *Foster and Carmack*, 1976]. DSW is formed on the continental shelf by regionally varying combinations of brine rejection from sea-ice growth and ocean-ice shelf interactions [*Kusahara et al*., 2011]. Coastal polynyas, areas of enhanced sea-ice production region driven by the interaction of strong winds and the "icescape", i.e., the local topography and glacial features, are directly linked to DSW formation [*Williams et al*., 2008]. *Tamura et al*. [2008] estimated sea-ice production in the majority of coastal polynyas around Antarctica and showed that the Ross Sea Polynya ($390 \pm 59\ km^3\ yr^{-1}$), the Cape Darnley Polynya ($181 \pm 19\ km^3\ yr^{-1}$) west of the Amery Ice Shelf, and the Mertz Polynya ($120 \pm 11\ km^3\ yr^{-1}$) off Adélie Land were the three most productive polynyas. While the Ross and Adélie polynyas had already been connected to AABW in the Australian-Antarctic Basin, the Cape Darnley result was new.

Recently, *Ohshima et al*. [2013] carried out mooring measurements off the Cape Darnley Polynya and found newly formed AABW, Cape Darnley Bottom Water, which ultimately contributes to AABW in the Atlantic Ocean. Previously, it had been thought that a wide continental shelf and/or large depression was necessary for the sufficient storage and salinification of DSW capable of producing AABW. However, *Ohshima et al*.

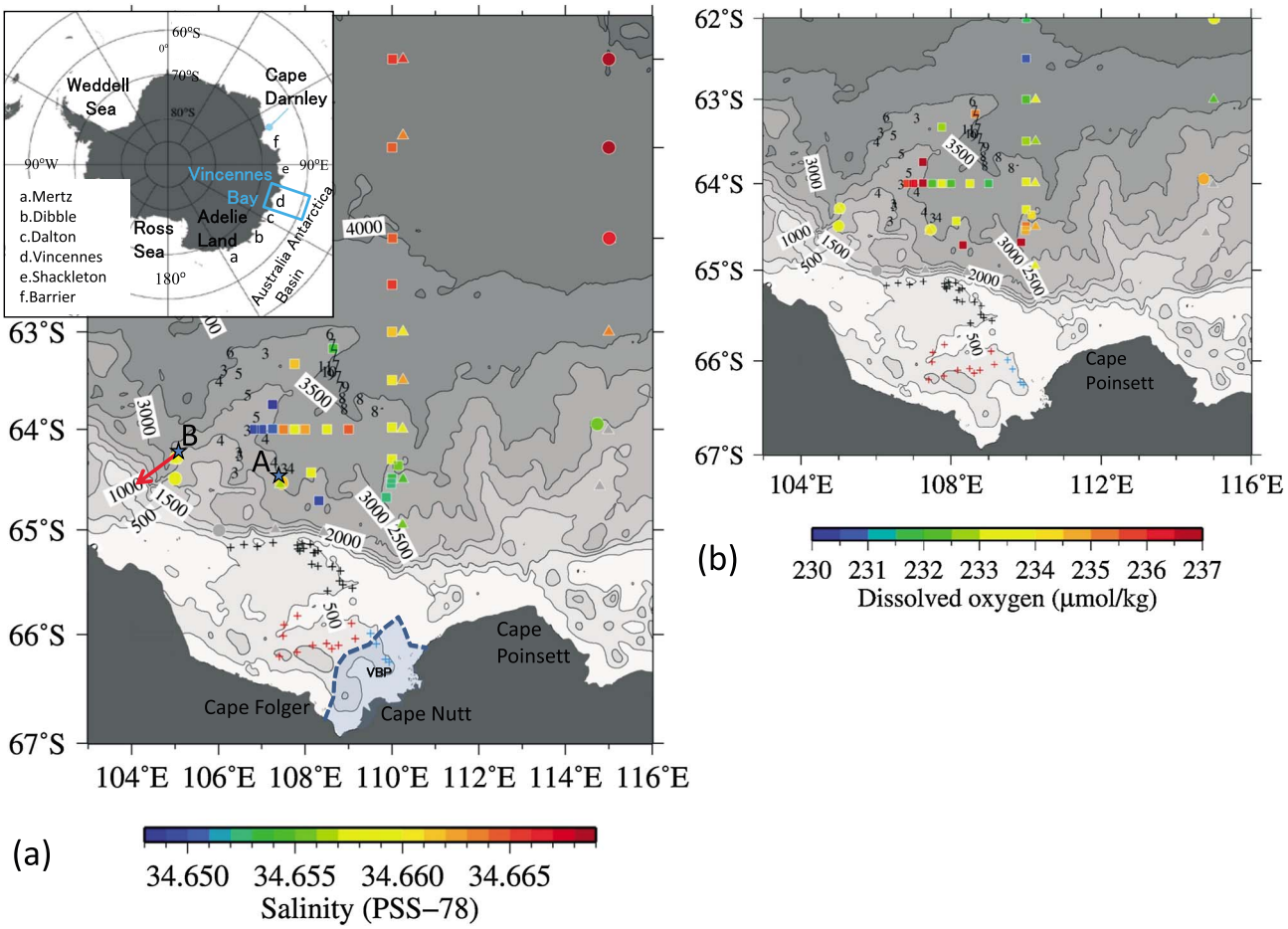

Figure 1. (a) A bathymetry map of the study region (ETOPO1: *Amante and Eakins* [2009]). Locations of hydrographic observations in 2011, 2012, and 2013 are indicated by circles, triangles, and squares, respectively. Along 110°E, the triangles representing the 2012 data locations are slightly offset to the east for clarity. Values of near-bottom salinity (averaged in the range of ±25 dbar of the neutral density surface of 28.32 kg m^{-3}) are indicated by colors. Mooring locations are indicated by stars with A and B. The red arrow indicates the averaged velocity at 120 m from the bottom at mooring B. Numbers from 5 to 12 indicate the months of observation and locations of the Argo floats. An area surrounded by the dashed line (~8900 km^2) indicates the Vincennes Bay Polynya (VBP) with sea-ice production > 5 m yr^{-1}. CTD data obtained by instrumented elephant seals near VBP in February and March are indicated by blue and red crosses, respectively, and obtained near the shelf break region in both months are indicated by black crosses. Inset map shows the location of the study area and polynya locations in the East Antarctica. (b) Same as in Figure 1a but for the values of dissolved oxygen.

[2013] showed that despite its relatively narrow shelf region, the enhanced sea-ice production in the Cape Darnley polynya was forming one of the most saline varieties of DSW around Antarctica. This has opened the door to the possibility of other polynya-based AABW sources, in particular in East Antarctica. While many of these are significantly smaller than the CDP in terms of annual sea-ice production [*Tamura et al.*, 2008], many have similar physical features.

The Vincennes Bay Polynya (VBP) forms every year in the coastal embayment southwest of Cape Poinsett (Figure 1) with sea-ice production of 73.3 ± 9.9 km^3 yr^{-1}, which ranks it as a "medium" class polynya relative to all polynyas around Antarctica [*Tamura et al.*, 2008]. A small depression exists over the continental shelf at the west of VBP, and sill depths from the depression to the continental slope are 500–600 m. The storage capacity of the depression is much smaller than the sizable Adélie Depression and with its modest amount of sea-ice production it has traditionally been ruled out as a source of DSW for AABW production. To the contrary, in this study we find strong evidence of AABW production from the VBP. Analyzing new mooring time series and hydrographic data, together with complementary data from instrumented seals, we identify the presence of newly formed AABW on the continental slope and link this to DSW forming in and around the VBP.

2. Observation and Data

We carried out mooring and hydrographic observations northeast of continental shelf off the Vincennes Bay (VB, Figure 1). While VB is technically defined between Cape Nutt and Cape Folger, in this paper we refer to the overall shelf region between 105 and 111°E as the VB region. Two moorings instrumented with conductivity-temperature recorders (Sea-Bird SBE37) and current meters (Aanderaa RCM-8/11) were deployed either side of a small ridge extending northeast from continental shelf at 105°E (mooring A: 64°31′S, 107°30′E, water depth of 3040 m; mooring B: 64°17′S, 105°02′E, water depth of 2880 m), from 2 January 2011 to 7 January 2012. These two locations were selected as the hypothesized pathway of DSW from the VBP. Conductivity and temperature data were obtained at 20 m above the bottom at both stations ($A = 3020$ m and $B = 2860$ m), and current data were obtained at 50 and 150 m above the bottom at mooring B (2830 and 2730 m).

Hydrographic observations using a conductivity, temperature, and depth profiler (Sea-Bird SBE911plus with SBE43) from the sea surface to 10 m above the bottom were also carried out off the VB in January 2011–2013 by TR/V *Umitaka-Maru* (Figure 1). Bottle samples were used for the calibration of conductivity by a salinometer (Guildline Autosal 8400B) and dissolved oxygen by an autotitration device. Furthermore, temperature and salinity data obtained by Argo autonomous floats (http://www.argo.ucsd.edu) and elephant seals, instrumented near Casey station in February 2012, were used to estimate the volume of locally formed DSW (Figure 1). The calibration procedure for the seal CTD data is described in *Roquet et al*. [2013, and references therein]. Accuracy of calibrated data is estimated to be ±0.01°C for temperature and ±0.02 in salinity. We also used ice production data estimated from heat flux calculation using the Special Sensor Microwave Imager Equal Area Scalable Earth Grid data by assuming that all of the heat loss at the surface is used for ice formation [*Tamura et al*., 2008, 2011].

3. Results

The mooring observations showed a distinct cooling and freshening in water mass properties from the onset of winter, providing the first direct evidence of newly ventilated AABW production in this region. The cold and fresh signals appeared in early June at mooring A (SG1 in Figure 2a) and a more intense signal appeared in late June (SG2). At mooring B, the moderate signal appeared about 20 days later in middle of July (SG3) and the more intense signal appeared in early August (SG4). The range of seasonal variations observed by these moorings at the depth around 3000 m off the VBP were about 0.01 in salinity, 0.1°C in temperature and 0.015 kg m^{-3} in neutral density. The cold and fresh water had neutral density larger than 28.33 (kg m^{-3}), and such conditions continued for about 5 months during winter through to midspring. Note that the cold and dense signal SG0 at mooring B was not associated with a significant salinity change. The onset and termination of the AABW signal was about 1 month later at mooring B where low-salinity signals were less prominent than at mooring A. We ascribe these signals to newly ventilated AABW from the downslope mixing of cold DSW exported from Vincennes Bay and down the ridge.

With the first observations of newly formed AABW confirmed off the VB from winter to spring, we now examine the relationship between the seasonal variations of the AABW signal (Figure 2a) and sea-ice production in the VBP (Figure 2b), as estimated from satellite data following *Tamura et al*. [2008]. In late June, about 3 months after the onset of sea-ice production in March, the first signal of new AABW (SG1) was observed at mooring A. The AABW signal finally weakened at mooring A in mid-November, nearly a fortnight after the end of sea-ice production. The timing and associated lags between these regions indicate a strong connection between the sea-ice production at VBP and outflow of newly formed AABW.

The water mass properties observed by the moorings, when compared in θ-S space with those obtained by the hydrographic observations at surrounding stations (Figure 3a), also point to the VBP as the origin of the AABW signal. Monthly averaged water properties at mooring A lie near a neutral density contour of 28.33 kg m^{-3} and are relatively constant from July to October. From the hydrographic data, there are two types of bottom water with different salinities. A denser, more saline variety exists below 3000 dbar on the continental rise which is similar to, and therefore likely derived from, the upstream mixture of new AABW from the Adélie region and AABW originally derived from the Ross Sea. In contrast, a fresher and less dense variety exists across the lower continental slope with depth range from 2500 to 3000 dbar west of

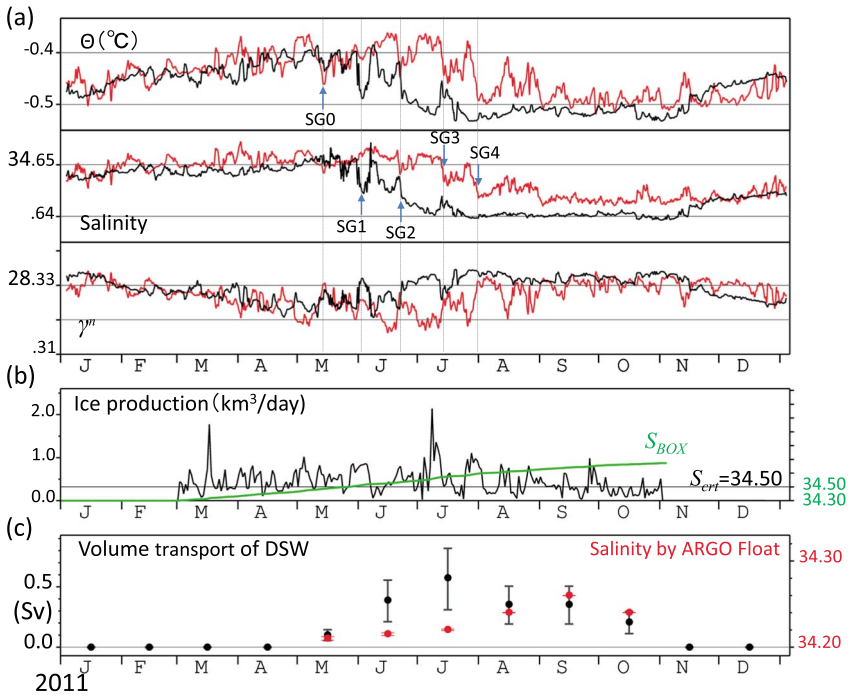

Figure 2. (a) Time series of potential temperature (°C), salinity, and neutral density (kg m^{-3}) obtained by moorings A (black line) and B (red line) from 2 January 2011 to 7 January 2012. The 25 h running average was applied to each time series. Arrows SG0-4 indicate the arrival of different water masses. (b) Time series of sea-ice production (black line) estimated from the satellite data [*Tamura et al.*, 2008]. The green line indicates the salinity calculated from the salinity flux associated with sea-ice production in VBP. (c) Volume transport of DSW for each month estimated from sea-ice production and its uncertainty. Salinities obtained by Argo float (red circle) were used in the estimation of the volume transport.

108°E (Figure 1a). The properties of the monthly averaged mooring data (black diamonds in Figure 3a) are similar to those of this fresher variety. The density at mooring A is denser than that at 3000 dbar of the offshore region (inversed triangles in Figure 3a) but lighter than the more saline and denser water mass at greater depth. Thus, the AABW produced from the VBP, while fresher and less dense than either Adélie or Ross AABW, nonetheless mixes into the upper layer of AABW in the Australian-Antarctic Basin.

Analysis of the hydrography with the time series of moored current observations further confirm the westward spread of a newly formed AABW from the VBP. Salinity values on the $\gamma^n = 28.32$ kg m^{-3} surface are lower around and west of 110°E than those along 115°E (Figure 1a). The dissolved oxygen concentration of the fresher bottom water is about 3 μmol kg^{-1} higher than that of saline one (Figure 1b). This result supports our assertion that DSW descends down from the VB, resulting in this signal. The averaged current velocity obtained at mooring B was about 0.15 m s^{-1} toward the southwest along the isobaths (red arrow in Figure 1a), which directly captured the westward spread. The velocity also explains the near 20 day time lag in the appearance of low-salinity signals between moorings A and B when considering their distance along the bottom contours.

The DSW source of this AABW was captured in temperature and salinity data collected by instrumented elephant seals on the continental shelf in VB during 2012. The DSW below 500 dbar near the VBP region is 34.49–34.51 in salinity and near the freezing point (blue and red diamonds and crosses in Figure 3b). The density of water with salinity $S > 34.50$ at freezing point is $\sigma_3 \approx 41.79$ kg m^{-3} and greater than density of AABW at 3000 dbar ($\sigma_3 \approx 41.73$kg m^{-3}, $\gamma^n \approx 28.334$kg m^{-3}). Examining the mooring data in θ-S space, we take the seasonal evolution line from fall (gray circle) to winter (gray star) and extrapolate it to the freezing point, where the salinity value would also be about 34.50. Furthermore, the modified Shelf Water (black diamonds in Figure 3b), which is a mixture between the DSW with around 34.50 in salinity and modified CDW (mCDW) around 500 dbar off the shelf edge, was observed by the instrumented seals at 500 dbar over the northern part of the continental shelf (the locations are shown by black crosses in Figure 1). Thus,

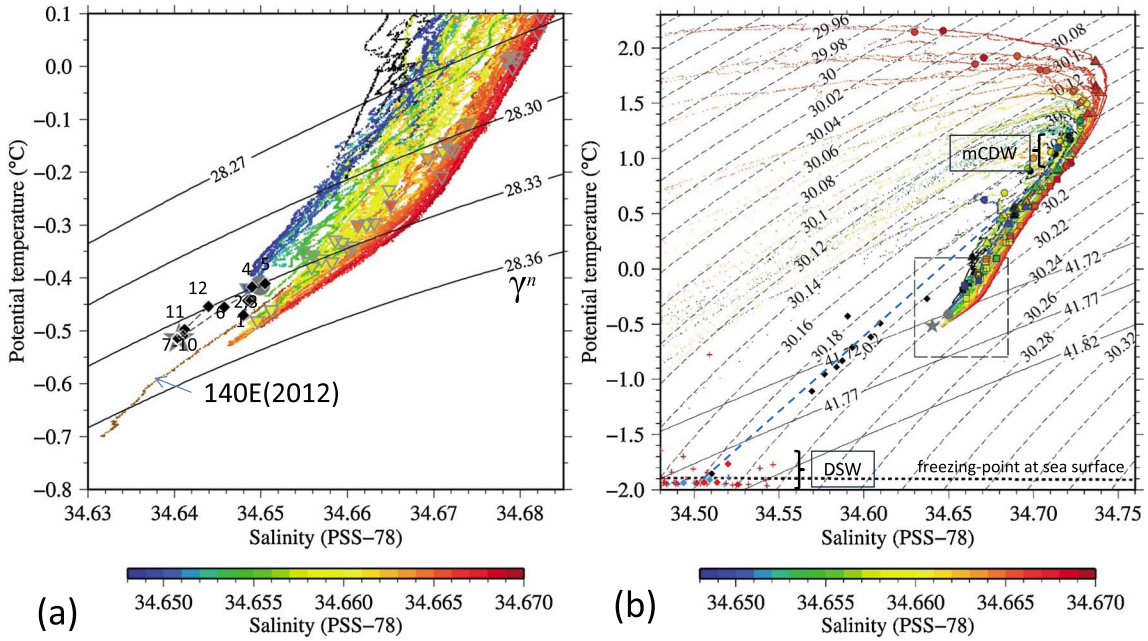

Figure 3. (a) θ-S diagram of bottom waters from the monthly averaged temperature and salinity obtained by mooring A and hydrographic data during 2011–2013. Averaged values are shown from July to October (gray stars) and from April to May (gray circles), respectively, and the monthly averaged values obtained at mooring A are shown with black diamonds and month labels. The black line denotes neutral density γ^n. As for the station symbol from Figure 1a, the θ-S profiles are color coded by salinity value, which is averaged in the range of ±25 dbar of neutral density of 28.32 kg m^{-3}. θ-S profiles indicated by a black dot are the stations where the neutral densities are less than 28.32 kg m^{-3} throughout the water column. Inversed triangles denote the values at 3000 dbar. Profiles obtained at 140°E in January 2012 are indicated by brown dots as a reference. (b) Similar to Figure 3a except with wider ranges. Values obtained by instrumented elephant seals on the continental shelf are indicated by diamond (500 dbar) and cross (other depth). The black diamonds indicate the stations near the shelf break region (locations are denoted by black crosses in Figure 1), and the blue and red diamonds indicate the stations near the VBP region (blue and red crosses in Figure 1). Dashed gray lines indicate potential density with respect to 500 dbar, while thin solid lines indicate σ_3. Gray star and circle are the same as that shown in Figure 3a. Circles, triangles, and squares in θ-S profiles denote the values at 500, 1000, and 2000 dbar, respectively.

the winter values of new AABW at mooring A (indicated by star in Figure 3) can be formed by mixing between the DSW and the ambient waters, as will be discussed in the following section.

4. The Mechanism of DSW Formation and AABW Production

Mooring observations have revealed that AABW originates from the VBP, East Antarctica. Time series of the mooring data at 3000 dbar, together with satellite-derived estimates of sea-ice production, shows that the first signal of the newly formed AABW appeared in June, about 3 months after the onset of sea-ice production.

Here let us consider multiple strands of observational evidence for the formation of DSW in VBP. The water properties of DSW below 500 dbar in February and March were almost uniform in the depression with $\theta \approx -1.9$°C and $S \approx 34.50$ (Figures 3b and S1). The potential pathway for DSW to be exported from the shelf region is through the northern part of the continental shelf and shelf edge regions with a minimum depth range of 500–600 m. The heaviest water formed in the previous winter is likely conserved in the water below 500 m in the depression as DSW. As there is likely to be some diffusion and mixing at these lower levels, we assume that these represent a conservative lower value for the maximum DSW produced in this region. We define the critical value of DSW salinity (S_{crt}) as the minimum required to provide sufficient negative buoyancy to flow down the continental slope and produce AABW. In this region we estimate S_{crt} to be 34.50, because the salinity in the depression is almost uniform around 34.50 below 500 m and roughly coincides with the salinity value from the extrapolation of θ-S line of the AABW at 3000 dbar and the near-bottom water (black diamond in Figure 3b) on the northern part of the continental shelf.

We also estimate the seasonal development of DSW salinity at VBP using a salt flux associated with satellite-derived sea-ice production. Following *Cavalieri and Martin* [1994], we estimated salinity flux induced by sea-ice production to be

$$\mathrm{SF} = (0.68 \times 0.001) S_{\mathrm{sfc}} \rho_{\mathrm{ice}} I_P, \tag{1}$$

where the S_{sfc} is the surface salinity, ρ_{ice} is the ice density, and the I_p is sea-ice production. We use the area of active sea-ice production greater than 5 m yr^{-1}, estimated to be about 8900 km^2 (shaded area shown in Figure 1), with an average depth of 500 m to calculate the change in salinity. We also assume that water temperature is at the freezing point at the onset of sea-ice production and that the salt rejected during sea-ice production immediately mixes through the water column in the box. Setting the initial salinity to 34.30, corresponding to the average value observed by the instrumented elephant seals in February and March in the upper 500 m, we estimate that the salinity in the box (S_{BOX}: green line in Figure 2b) reaches the previously determined critical value of salinity ($S_{\mathrm{crt}} = 34.50$) at the end of May. This supports the mechanism of DSW formation with sufficient salinity to produce AABW.

5. Estimation of AABW Transport

Here we estimate the DSW volume transport to examine the contribution of AABW from the VBP to other regions. Considering the contour line of σ_3, and the thermobaric effect, DSW with salinity of 34.50 now has an equivalent density to that at 3000 dbar (Figure 3). As discussed in the previous section, it is reasonable to assume that the DSW starts to sink down the slope when its value at the density front across the shelf edge reaches the critical salinity, S_{crt}. Since the salinity flux caused by sea-ice production modifies fresh surface water flowing into the bay, we can estimate the transport of fresh surface water inflow based on the conservation of total salt amount. In addition, we also assume that the inflow transport is equal to the outflow based on the conservation of volume. In this model, assuming that the entire salinity flux is mixed with fresh surface water inflow to form DSW, we can estimate an upper limit of DSW transport. With these assumptions, the volume transport U is estimated by

$$U = \frac{\mathrm{SF}\rho_{\mathrm{DSW}}}{S_{\mathrm{crt}}\rho_{\mathrm{DSW}} - S_{\mathrm{out}}\rho_{\mathrm{out}}}. \tag{2}$$

In equation (2), ρ_{DSW} is the density of DSW and S_{out} and ρ_{out} are the salinity and density in the regions outside of the VB, respectively. For S_{out} and ρ_{out}, the Argo float data for each month (Figure 1) are used. The monthly transport values were estimated by equation (1) after the salinity in the box reaches S_{crt}.

The estimated volume transport has the maximum of 0.56 ± 0.25 Sv in July (Figure 2c). The error associated with this transport is estimated from that of the sea-ice production data (±25% by *Tamura et al*. [2008]) and the standard deviation of averaged salinity obtained in each month by Argo float. There is no transport during fall because despite active sea-ice production, the salinity in the box is yet to exceed the critical salinity. The annual averaged DSW transport is 0.16 ± 0.07 Sv. If we assume end point values of modified Circumpolar Deep Water (mCDW) as 1.05°C in temperature (Figure 3b) as discussed by *Ohshima et al*. [2013], the AABW off VBP would be formed by mixing of DSW and mCDW with a ratio of roughly 1:1 from the temperature as indicated by dashed blue line in Figure 3b. Thus, the AABW transport is estimated to be 0.32 ± 0.14 Sv. Although these estimates should be regarded as the upper bounds of the AABW volume, they can reach as much as 20% of those from Adélie Depression [*Rintoul*, 1998; *Williams et al*., 2010].

6. Conclusions

The VBP is a medium-sized polynya, capable of forming AABW. This AABW source is somewhat weaker than other key area, and the originated AABW variety may not be dense enough to reach the true abyssal plain. Nonetheless, it can be considered an important contribution to the upper and intermediate layer of the AABW in the Australian-Antarctic Basin.

The discovery of newly ventilated AABW off the VBP confirms that the formation regions of AABW are widespread. Besides Mertz Polynya, there are at least two of similar or larger size polynyas (Shackleton and Dibble as shown in inset of Figure 1a) along the coast facing the Australian-Antarctic Basin [*Tamura et al*., 2008]. Barrier Polynya is another candidate of similar production, which is located between Shackleton

and Cape Darnley Polynyas. Given the dramatic changes to regional and total AABW properties observed over recent decades [*Aoki et al*., 2005, 2013; *Rintoul*, 2007; *Johnson et al*., 2008; *Jacobs and Giulivi*, 2010; *Shimada et al*., 2012; *Purkey and Johnson*, 2013], the assessment and monitoring of all source regions is needed and should include medium-sized polynyas like the VBP which will be the most sensitive to change.

Acknowledgments

We are deeply indebted to the officers, crew, and scientists on board TR/V *Umitaka-maru*. This work was supported by JSPS KAKENHI grants 23310003, 25241001, and 23340135, MEXT for physical and chemical oceanographic observations under Japanese Antarctic Research Expedition, and the Australian Government's Cooperative Research Centres Programme through the Antarctic Climate and Ecosystem Cooperative Research Centre. IMOS seal CTD data were provided through the Australian Animal Tracking and Monitoring System, a facility of Integrated Marine Observing System.

The Editor thanks two anonymous reviewers for their assistance in evaluating this paper.

References

Amante, C., and B. W. Eakins (2009), ETOPO1: 1 Arc-Minute Global Relief Model: Procedures, data sources and analysis, *NOAA Technical Memorandum NESDIS NGDC-24*, National Geophysical Data Center, Boulder, Colo.

Aoki, S., S. R. Rintoul, S. Ushio, S. Watanabe, and N. L. Bindoff (2005), Freshening of the Adélie Land Bottom Water near 140°E, *Geophys. Res. Lett.*, *32*, L23601, doi:10.1029/2005GL024246.

Aoki, S., Y. Kitade, K. Shimada, K. I. Ohshima, T. Tamura, C. C. Bajish, M. Moteki, and S. R. Rintoul (2013), Widespread freshening in the seasonal ice zone near 140°E off the Adelie Land Coast, Antarctica, from 1994 to 2012, *J. Geophys. Res. Oceans*, *118*, 6046–6063, doi:10.1002/2013JC0090009.

Cavalieri, D. J., and S. Martin (1994), The contribution of Alaskan, Siberian, and Canadian coastal polynyas to the cold halocline layer of the Arctic Ocean, *J. Geophys. Res.*, *99*, 18,343–18,362, doi:10.1029/94JC01169.

Foster, T. D., and E. C. Carmack (1976), Frontal zone mixing and Antarctic Bottom Water formation in the southern Weddell Sea, *Deep-Sea Res.*, *23*, 301–317.

Gill, A. E. (1973), Circulation and bottom water production in the Weddell Sea, *Deep-Sea Res.*, *20*, 111–140.

Jacobs, S. S. (2004), Bottom water production and its links with the thermohaline circulation, *Antarct. Sci.*, *16*, 427–437.

Jacobs, S. S., and C. F. Giulivi (2010), Large multidecadal salinity trends near the Pacific-Antarctic continental margin, *J. Clim.*, *23*, 4508–4524, doi:10.1175/2010JCLI3284.1.

Jacobs, S. S., A. F. Amos, and P. M. Bruchausen (1970), Ross Sea oceanography and Antarctic Bottom Water formation, *Deep-Sea Res.*, *17*, 935–962.

Johnson, G. C., S. G. Purkey, and J. L. Bullister (2008), Warming and freshening in the Abyssal Southeastern Indian Ocean, *J. Clim.*, *21*, 5351–5363.

Kusahara, K., H. Hasumi, and G. D. Williams (2011), Dense shelf water formation and brine-driven circulation in the Adelie and George V Land region, *Ocean Modell.*, *37*, 122–138.

Marshall, J., and K. Speer (2012), Closure of the meridional overturning circulation through Southern Ocean upwelling, *Nat. Geosci.*, doi:10.1038/NGEO1391.

Ohshima, K. I., et al. (2013), Antarctic Bottom Water production by intense sea-ice formation in the Cape Darnley polynya, *Nat. Geosci.*, doi:10.1038/NGEO1738.

Purkey, S. G., and G. C. Johnson (2013), Antarctic Bottom Water warming and freshening: Contributions to sea level rise, ocean freshwater budgets, and global heat gain, *J. Clim.*, *26*, 6105–6122, doi:10.1175/JCLI-D-12-00834.1.

Rintoul, S. R. (1998), On the origin and influence of Adélie Land Bottom Water, Ocean, Ice and Atmosphere: Interactions at Antarctic Continental Margin, *Antarct. Res. Ser.*, *75*, 151–171.

Rintoul, S. R. (2007), Rapid freshening of Antarctic Bottom Water formed in the Indian and Pacific oceans, *Geophys. Res. Lett.*, *34*, L06606, doi:10.1029/2006GL028550l.

Roquet, F., et al. (2013), Estimates of the Southern Ocean general circulation improved by animal-borne instruments, *Geophys. Res. Lett.*, *40*, 1–5, doi:10.1029/2012GL054022.

Shimada, K., S. Aoki, K. I. Ohshima, and S. R. Rintoul (2012), Influence of Ross Sea Bottom Water changes on the warming and freshening of the Antarctic Bottom Water in the Australian-Antarctic Basin, *Ocean Sci.*, *8*, 419–432.

Speer, K., S. R. Rintoul, and B. Sloyan (2000), The diabatic Deacon cell, *J. Phys. Oceanogr.*, *30*, 3212–3222.

Tamura, T., K. I. Ohshima, and S. Nihashi (2008), Mapping of sea-ice production for Antarctic coastal polynyas, *Geophys. Res. Lett.*, *35*, L07606, doi:10.1029/2007GL032903.

Tamura, T., K. I. Ohshima, S. Nihashi, and H. Hasumi (2011), Estimation of surface heat/salt fluxes associated with sea ice growth/melt in the Southern Ocean, *Sci. Online Lett. Atmos.*, *7*, 17–20, doi:10.2151/sola.2011-005.

Williams, G. D., N. L. Bindoff, S. J. Marsland, and S. R. Rintoul (2008), Formation and export of dense shelf water from the Adélie Depression, East Antarctica, *J. Geophys. Res.*, *113*, C04039, doi:10.1029/2007JC004346.

Williams, G. D., S. Aoki, S. S. Jacobs, S. R. Rintoul, T. Tamura, and N. L. Bindoff (2010), Antarctic Bottom Water from the Adélie and George V Land coast, East Antarctica (140–149°E), *J. Geophys. Res.*, *115*, C04027, doi:10.1029/2009JC005812.